

# A Modified Method Based on the Discrete Sliding Norm Transform to Reduce the PAPR in OFDM Systems

R. Salmanzadeh and B. Mozaffari Tazehkand

Orthogonal frequency division multiplexing (OFDM) is a modulation technique that allows the transmission of high data rates over wideband radio channels subject to frequency selective fading by dividing the data into several narrowband and flat fading channels. OFDM has high spectral efficiency and channel robustness. However, a major drawback of OFDM is that the peak-to-average power ratio (PAPR) of the transmitted signals is high, which causes nonlinear distortion in the received data and reduces the efficiency of the high power amplifier in the transmitter. The most straightforward method to solve this problem is to use a nonlinear mapping algorithm to transform the signal into a new signal that has a smaller PAPR. One of the latest nonlinear methods proposed to reduce the PAPR is the  $L_2$ -by-3 algorithm, which is based on the discrete sliding norm transform. In this paper, a new algorithm based on the  $L_2$ -by-3 method is proposed. The proposed method is very simple and has a low complexity analysis. Simulation results show that the proposed method performs better, has better power spectral density, and is less sensitive to the modulation type and number of subcarriers than  $L_2$ -by-3.

**Keywords:** OFDM symbols, discrete sliding norm transform, DSNT, PAPR reduction, spectral density.

## I. Introduction

Orthogonal frequency division multiplexing (OFDM) has been widely used in digital audio and video broadcasting systems and high-speed communication networks. OFDM is a multicarrier modulation method that converts a high data rate stream into a number of lower data rate streams, which are transmitted simultaneously over a number of narrowband flat channels using well-known subcarriers. In fact, to reduce the data rate, we need to increase the interval time of the symbol duration to reduce the inter symbol interference (ISI), which is caused by multipath fading. The ISI can be almost completely eliminated by using the cyclic prefix (CP), which is a guard interval. The main advantages of OFDM are its high bandwidth efficiency, robustness to multipath fading, simplification of channel equalization, and low computational complexity based on using the fast Fourier transform (FFT) technique [1]. The major drawback of OFDM is its high peak-to-average power ratio (PAPR). High PAPR causes a severe distortion in both in-band and out-of-band when the OFDM signal passes through a nonlinear high power amplifier (HPA). To prevent this, the amplifier must be biased in its linear region, which means the linear region has a large range. Such an amplifier carries with it many costs, and its power efficiency is very low. Therefore, to obtain an efficient PAPR, reduction of the transmitted signal is necessary.

Several methods have been proposed for reducing the PAPR parameter, including selected mapping (SLM) [2], [3], partial transmit sequence (PTS) [4], [5], clipping and filtering [6], [7], tone reservation (TR) and tone injection (TI) [8], active

Manuscript received Jan.13, 2013; revised Apr. 5, 2013; accepted Apr. 15, 2013.

This work was supported by the ITRC with grant number as T/15705/500, Iran.

R. Salmanzadeh (phone: +98 4113393788, r\_salmanzadeh89@msc.tabrizu.ac.ir) and B. Mozaffari Tazehkand (corresponding author, mozaffary@tabrizu.ac.ir) are with the Department of Electrical and Computer, University of Tabriz, Tabriz, Iran.

constellation extension (ACE) [9], [10], block coding [11], [12], and such nonlinear methods as clipping and companding [13]-[15]. PAPR reduction is achieved by the above-mentioned methods at the expense of a decrease in data rate and transmit signal power and an increase in computational complexity and bit error rate (BER). For example, in the TR, TI, and ACE algorithms, the power level in the transmit signal must increase after the PAPR reduction. Side information is required in SLM and PTS that must be sent to the receiver. Therefore, extra power consumption and loss in data rate are the results. The complexity is increased at both the transmitter and the receiver for the following methods: coding, PTS, SLM, interleaving, TR, and TI. Each of these methods has different PAPR reduction capability and computational complexity. It is important to analyze the power saving in the PA owing to PAPR reduction and the power consumption during implementation resulting from computational complexity [16].

The most straightforward method for reducing the PAPR of the transmitted signal is using a nonlinear mapping algorithm. One of the most recently introduced nonlinear functions is the  $L_2$ -by-3 transform proposed by Dursun and Grigoryan [17]. This algorithm is based on the discrete sliding norm transform (DSNT); it uses three samples for every transform and introduces a controlling parameter,  $\alpha$ , which can adjust the PAPR of the output signal.

In this paper, we propose a new mapping algorithm based on the  $L_2$ -by-3 method that is simpler in terms of the transmitter and receiver and has a lower PAPR and more efficient power spectral density (PSD). The proposed algorithm introduces another parameter,  $\beta$ , which can control the PAPR parameter, PSD, and symbol error rate (SER) in the output signal.

The paper is organized as follows. In section II, the OFDM system, the PAPR, the complementary cumulative distribution function (CCDF), and the Rapp model for HPAs are reviewed. In section III, the  $L_2$ -by-3 technique is considered, abstractly. The proposed method is introduced in section IV, and the simulation results are shown in section V. Finally, in section VI, the complexity of the proposed algorithm is analyzed.

## II. Overview of OFDM System Parameters

### 1. OFDM Systems

The OFDM technique converts a frequency selective channel into a number of frequency flat channels by dividing the available spectrum into a number of overlapping and orthogonal narrowband subchannels, and each of them independently sends its own data using a subcarrier. A block diagram of the OFDM system in a baseband model is shown in Fig. 1.

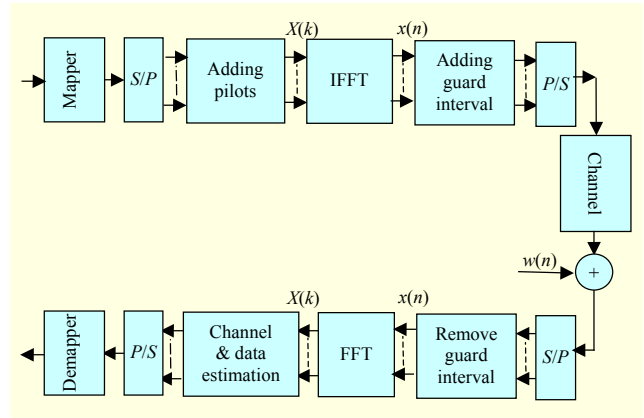


Fig. 1. OFDM system in baseband model.

In the transmitter, the binary inputs are first grouped to obtain a symbol in the  $M$ -ary baseband. According to a predefined baseband modulation, such as quadrature phase shift keying (QPSK) or  $M$ -ary quadrature amplitude modulation (MQAM) with  $M = 16$ ,  $M = 64$ ,  $M = 256$ , and so on, the obtained symbols are modulated using a signal mapper subsystem. In the next step, an  $S/P$  subblock converts the serial input symbols into a data block as a vector form, which can be denoted as follows:  $X = [X_0 X_1 \dots X_{N-1}]$ . The size of the data vector is " $N$ ," which represents the number of subcarriers in the OFDM signal. Each subcarrier is modulated by the obtained symbols in the data vector using the inverse FFT (IFFT) algorithm, and the time domain of the OFDM signal is consequently calculated as follows:

$$x(n) = \frac{1}{\sqrt{N}} \sum_{k=0}^{LN-1} X_k e^{j \frac{2\pi kn}{LN}}, \quad 0 \leq n \leq LN-1, \quad (1)$$

where " $L$ " is an oversampling factor, which can be set to 2, 4, 8, or 16 [8]. Because of nonlinear mapping, in this paper, we choose  $L = 16$  to more accurately obtain the PSD and CCDF parameter. Also, oversampling is done with zero padding. To prevent the effect of ISI in OFDM signals, a guard time, well known as the CP, must be added to it. The adding process is shown in Fig. 2.

Finally, the obtained OFDM signal is converted to serial form and is transmitted to the receiver through a frequency selective channel, which is often considered a Rayleigh fading model with additive white Gaussian noise (AWGN). The

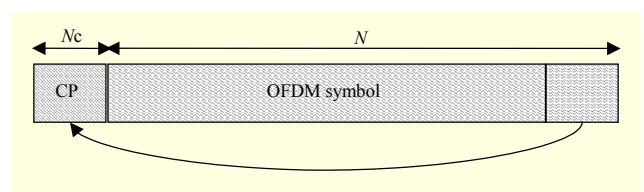


Fig. 2. OFDM symbol after cyclic prefix addition.

signal obtained by the receiver after removing the CP is demodulated, and the data is recovered based on the estimated channel. In this paper, it is assumed that there is no synchronization error.

## 2. PAPR Parameter

The PAPR of a signal,  $x(n)$ , is defined by (2), which explains the ratio of peak power with respect to the power average.

$$PAPR = \frac{\max_{0 \leq n \leq LN-1} |x(n)|^2}{E |x(n)|^2}, \quad (2)$$

where  $E\{\cdot\}$  indicates the expectation of the signal. Usually, an oversampling factor ( $L=2, L=4, L=8, \text{ or } L=16$ ) is used to estimate the actual PAPR based on its discrete samples. To evaluate the PAPR performance accurately, statistically speaking, the CCDF of the PAPR is used to describe the probability of a large deviation event with respect to the expected value as a given threshold, such as  $PAPR_0$ . The CCDF function can be written as follows:

$$CCDF = \Pr(PAPR \geq PAPR_0). \quad (3)$$

In multicarrier systems, anyone can obtain a simple approximate expression of the CCDF of the PAPR parameter using the Nyquist rate sampling theorem. From the central limit theorem, the real and imaginary parts of the time domain signal samples can be Gaussian distributions, each with zero mean and variance  $\sigma^2$  for an OFDM symbol when there are a large number of subcarriers. Equation (4) shows the related parameters.

$$\begin{aligned} x(n) &= x_r(n) + jx_i(n), \quad n = 0, 1, \dots, N-1, \\ f_r(x) &= f_i(x) = \frac{1}{\sqrt{2\pi\sigma^2}} e^{-\frac{x^2}{2\sigma^2}}. \end{aligned} \quad (4)$$

Therefore, the instantaneous power of the OFDM signal follows exponential distribution. The CDF of the amplitude of a signal sample is given by the following:

$$\begin{aligned} |x(n)| &= \sqrt{x_r^2 + x_i^2}, \quad n = 0, 1, \dots, N-1, \\ z(n) &= |x(n)|^2, \\ f_z(z) &= \frac{1}{2\sigma^2} e^{-\frac{z}{2\sigma^2}}, \quad z \geq 0. \end{aligned} \quad (5)$$

Finally, the CCDF can be written as follows if it is assumed that any sample in a multicarrier signal is independent and identically distributed.

$$\begin{aligned} p(PAPR > PAPR_0) &= 1 - p(PAPR \leq PAPR_0) \\ &= 1 - p(z(0) \leq PAPR_0, \dots, z(N-1) \leq PAPR_0) \\ &= 1 - \prod_{n=0}^{N-1} p(z(n) \leq PAPR_0) = 1 - (1 - e^{-\frac{PAPR_0}{2\sigma^2}})^N. \end{aligned} \quad (6)$$

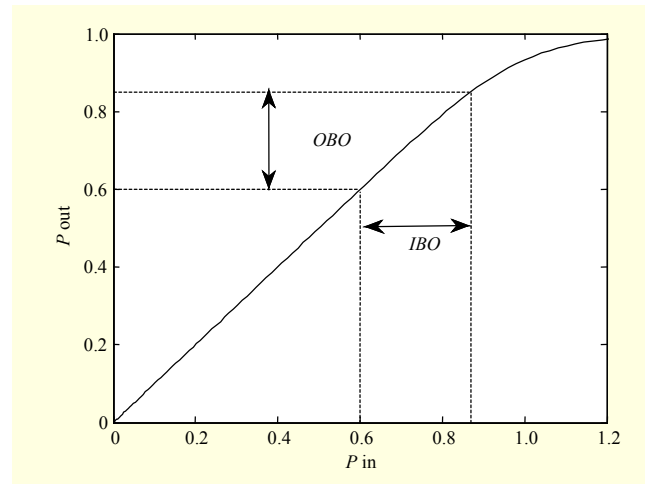


Fig. 3. AM/AM characteristic of HPA using Rapp model,  $s=10$ ,  $V_{sat}=1$ .

## 3. High Power Amplifier Effects in OFDM Systems

When a multicarrier signal passes through a nonlinear device, such as an HPA or a digital-to-analog converter (DAC), a higher peak in input signal generates out-of-band energy and in-band distortion. These effects can severely degrade the system performance. The nonlinear behavior of an HPA can be modeled as two characteristics: AM/AM and AM/PM. There are many methods that can be used to model the distortion caused by an HPA, including the Saleh, Gorbani, and Rapp models. Figure 3 shows the Rapp model, which can be calculated using (7). This equation models a typical AM/AM distortion only.

$$V_{out} = \frac{V_{in}}{(1 + (\frac{V_{in}}{V_{sat}})^{2s})^{\frac{1}{2s}}}, \quad (7)$$

where  $V_{in}$  is the input signal,  $V_{out}$  is the output signal and  $V_{sat}$  is the maximum input signal, which causes the saturation effect in the nonlinear PA and “ $s$ ” is the smoothing factor that controls the nonlinearity of the amplifier.

In this figure, the associated input backoff (IBO) and output backoff (OBO) regions are also shown. The amount of the IBO parameter can be controlled by peak power and the average power of the input signal. Otherwise, to decrease the nonlinear effects of an HPA, a signal with high peak power must be backed off to the linear region of the HPA by decreasing the average power of the input signal, but it degrades the power efficiency of the HPA. The IBO parameter can be defined as

$$IBO = 10 \log\left(\frac{P_{max}}{P_{in}}\right), \quad (8)$$

where  $P_{\max}$  is the peak power or the maximum power of the input signal and also  $P_{\text{in}}$  is the average power of the signal. If the PAPR parameter of the signal is lower than the IBO, then the performance of the HPA can be efficiently increased. Therefore, we need an algorithm that can decrease the PAPR parameter.

Clearly, it would be desirable to have the average and peak power values as close to one another as possible to maximize the efficiency of the HPA. In addition, to the large burden placed on the HPA, a high PAPR requires high resolution for both the transmitter's DAC and the receiver's analog-to-digital converter (ADC), since the dynamic range of the signal is proportional to the PAPR. High resolution in digital-to-analog and analog-to-digital conversion requires additional complexity, cost, and power burden on the system.

### III. Overview of the Dursun method ( $L_2$ -by-3)

In this section,  $L_2$ -by-3, which is the nonlinear algorithm first proposed by Dursun is reviewed [17]. First, we introduce the general definition of DSNT.

Let  $x$  be a real vector with  $N$  samples denoted by  $x = [x_0 \ x_1 \ \dots \ x_{N-1}]^T$ . A nonlinear discrete transform, as shown in (9), converts real vector value " $x$ " into " $y$ ," another real vector value.

$$y_n = \begin{cases} x_0, & n = 0, \\ \frac{x_n}{\sqrt{\sum_{k=0}^n x_k^2}}, & n = 1, 2, \dots, N-1. \end{cases} \quad (9)$$

The above transform is called the discrete  $L_2$ -sliding norm transform ( $L_2$ -DSNT). The  $L_2$ -by-3 transform is a particular kind of DSNT method based on the  $L_2$  metric. It uses three samples,  $x_{n-1}$ ,  $x_n$ ,  $x_{n+1}$ , in each sliding window to calculate the output samples. The following equation shows the  $L_2$ -by-3

mapping algorithm.

$$y_n = \frac{x_n}{\sqrt{\alpha + x_{(n-1)_N}^2 + x_{(n)_N}^2 + x_{(n+1)_N}^2}}, \quad (10)$$

where  $(\cdot)_N$  denotes the modulo  $N$  operation: if  $n = 0$ , then  $x_{n-1} = x_{N-1}$ , which can be simplified as  $x_{N-1}$  in modulo  $N$ ; if  $n = N-1$ , then  $x_{n+1} = x_N = x_0$  and  $0 \leq \alpha \leq 1$ , which can control the value of the PAPR parameter. It is clear from (10) that if  $x_n = 0$ , then there is no need to calculate  $y_n$  because  $y_n = x_n = 0$ .

This transform is reversible, and anyone can obtain the non-zero original data through (11).

$$\begin{bmatrix} \Delta_0 & 1 & 0 & 0 & 0 & 1 \\ 1 & \Delta_1 & 1 & 0 & 0 & 0 \\ 0 & 1 & \Delta_2 & 1 & 0 & 0 \\ \cdot & \cdot & \cdot & \cdot & \cdot & \cdot \\ 0 & 0 & 0 & 1 & \Delta_{N-2} & 1 \\ 1 & 0 & 0 & 0 & 1 & \Delta_{N-1} \end{bmatrix} \begin{bmatrix} x_0^2 \\ x_1^2 \\ x_2^2 \\ \cdot \\ x_{N-2}^2 \\ x_{N-1}^2 \end{bmatrix} = -\alpha \begin{bmatrix} 1 \\ 1 \\ 1 \\ 1 \\ 1 \\ 1 \end{bmatrix} \quad (11)$$

$$\Delta_n = 1 - \frac{1}{y_n^2}, \quad n = 0, 1, \dots, N-1.$$

The result obtained using (11) is the squared value of any non-zero data as denoted by  $x_n^2$  and must be converted to the original data as  $x_n$  using (12).

$$x_n = \sqrt{x_n^2} \text{sgn}(y_n), \quad (12)$$

where " $\text{sgn}(\cdot)$ " is the sign function.

The CCDF of the PAPR parameter in the  $L_2$ -by-3 method is shown in Fig. (4), based on a 16QAM modulation with  $N = 64$  and different values of parameter  $\alpha$ . As shown in the figure, when the value of parameter  $\alpha$  is increased, the PAPR parameter is also increased. Also, as shown in Fig. 5, when parameter  $\alpha$  decreases, the performance of PSD degrades.

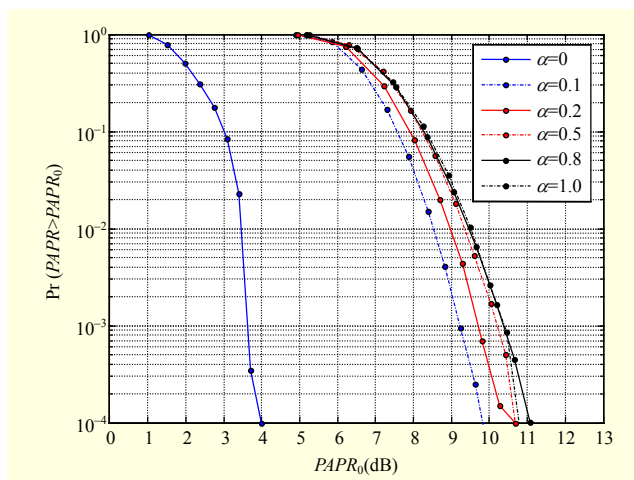


Fig. 4. PAPR in  $L_2$ -by-3;  $N=64$ , 16QAM,  $L=16$ .

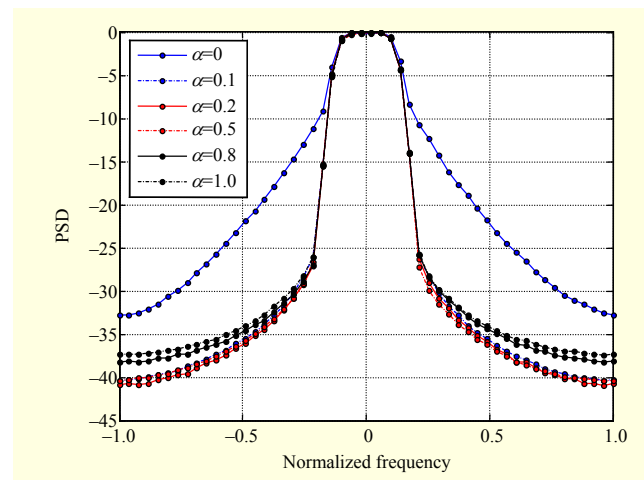


Fig. 5. PSD in  $L_2$ -by-3;  $N=64$ , 16QAM, and  $L=16$ .

#### IV. Proposed Method

In this paper, the modified sliding norm transform (MSNT), which is a new nonlinear algorithm based on the  $L_2$ -by-3 method with some modifications, is proposed. The MSNT algorithm has a better PAPR reduction performance and less complexity both on the transmitter and receiver side. A corresponding block diagram of the transmitter side is shown in Fig. 6.

$L_2$ -by-3 uses three samples (that is,  $x_{n-1}$ ,  $x_n$ , and  $x_{n+1}$ ) in every sliding window to calculate an output sample and introduces parameter  $\alpha$  ( $0 \leq \alpha \leq 1$ ) to control the PAPR and PSD parameters in the output signal. MSNT is based on the  $L_2$ -by-3 method, but it uses only two complex value samples ( $x_{n-1}$  and  $x_n$ ) and their absolute values in any sliding window, so it is clear that the computational complexity is less than that of the  $L_2$ -by-3 method. In our algorithm, in addition to parameter  $\alpha$ , parameter  $\beta$  ( $1 \leq \beta \leq 10$ ) is applied to adjust the PAPR and PSD parameters in the output signal. The proposed nonlinear mapping function is defined as follows:

$$y_n = \begin{cases} x_n, & n = 0, \\ \frac{x_n}{\sqrt{\alpha + \beta \cdot |x_{(n)}|^2 + |x_{(n-1)}|^2}}, & n = 1, 2, \dots, N-1. \end{cases} \quad (13)$$

According to Fig. 6, the input data is first modulated by one of the digital modulation technique (QPSK, 16QAM, 64QAM, and so on). The obtained modulated data is grouped to a set with  $N$  symbols to get the data of  $N$  subcarriers to calculate the OFDM symbol according to the IFFT module. In the next step, the MSNT is applied to the obtained signal, denoted by  $x(n) = [x_0 \ x_1 \ \dots \ x_{N-1}]^T$ , using (13). To further reduce the PAPR, we reverse the frame obtained in the previous step and then apply the MSNT again, which is shown in Fig. 7. Finally, the calculated signal is converted to serial form and then passed through the DAC and HPA.

To reconstruct the original data on the receiver side, we must do the reverse operation, which is done on the transmitter side.

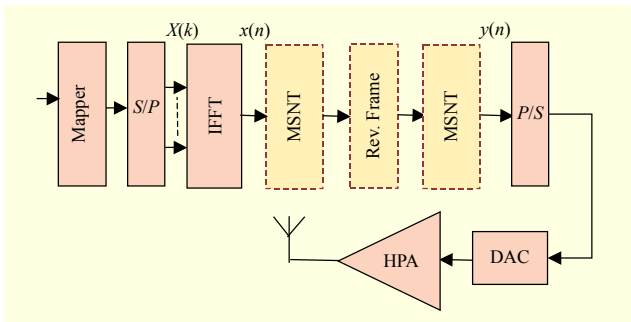


Fig. 6. Block diagram of MSNT.

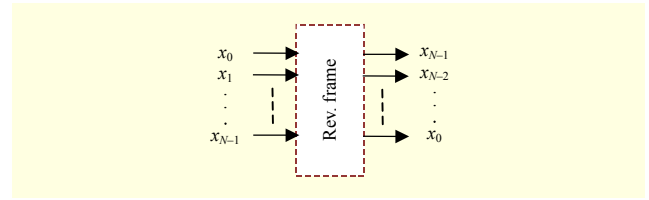


Fig. 7. Block diagram of frame reversing in MSNT.

First, it is necessary to verify that the MSNT algorithm is reversible. The proposed transform is reversible and so anyone can compute the  $x_n$  using  $x_{n-1}$  and the currently received input sample as  $y_n$ , based on (14), which can be obtained by modifying (13). Also, using (13), it is clear that when  $x_n = 0$ ,  $y_n = 0$ , and the corresponding input and output samples always have the same sign.

$$\begin{aligned} y_n &= \frac{x_n}{\sqrt{\alpha + \beta \cdot |x_n|^2 + |x_{n-1}|^2}} \\ \Rightarrow |y_n|^2 &= \frac{|x_n|^2}{\alpha + \beta \cdot |x_n|^2 + |x_{n-1}|^2} \\ \Rightarrow |x_n|^2 (\beta \cdot |y_n|^2 - 1) &= -|y_n|^2 (\alpha + |x_{n-1}|^2). \quad (14) \\ \Rightarrow |x_n|^2 &= \frac{|y_n|^2 (\alpha + |x_{n-1}|^2)}{1 - \beta \cdot |y_n|^2} \\ x_n &= y_n \cdot \sqrt{\frac{\alpha + |x_{n-1}|^2}{1 - \beta \cdot |y_n|^2}} \end{aligned}$$

Therefore, we can simplify the obtained results as follows:

$$x_n = \begin{cases} y_0 & y_n \neq 0, n = 0, \\ y_n \cdot \sqrt{\frac{\alpha + |x_{n-1}|^2}{1 - \beta \cdot |y_n|^2}} & y_n \neq 0, n = 1, 2, \dots, N-1, \\ 0 & y_n = 0. \end{cases} \quad (15)$$

#### V. Simulation Results

In this section, we show simulation results to evaluate the performance of MSNT and compare MSNT with the conventional OFDM and  $L_2$ -by-3 methods. Table 1 shows the parameters used in all simulations.

Figure 8 shows the PAPR reduction performance of MSNT with different values of  $\alpha$  and where  $\beta = 10$ , and the baseband modulation is 64QAM and  $N = 64$ . It is shown that increasing  $\alpha$  from 0.1 to 1 controls the PAPR of the output signal from 2.5 dB to 10 dB when we have a threshold probability of  $10^{-4}$ . Also, the PSD of MSNT, computed by the Welch algorithm, is shown in Fig. 9. When parameter  $\alpha$  changes, the corresponding PSD ceases to change. In other words, the PSD is not more sensitive with respect to variations of parameter  $\alpha$ .

In the next step, we investigate the performance of MSNT



Table 1. List of used parameters in all simulations.

Parameters	Values of parameters
Type of baseband modulations	QPSK, 16QAM, 64QAM, 128QAM
Number of subcarriers	$N = 64, 128, 256$
Algorithms	Conventional OFDM $L_2$ -by-3 MSNT
Values of $\beta$ parameter	$1 \leq \beta \leq 10$
Values of $\alpha$ parameter	$0 \leq \alpha \leq 1$
Number of OFDM symbols	10,000 for PAPR and CCDF, 500 for SER 500 OFDM symbols = $500 \times (N = 64) = 32,000$ data symbol
Calculation of PSD	Welch algorithm

with variations of  $\beta$  in the range, as in [1], [9]. The CCDF of the PAPR is shown in Fig. 10. It is shown that when parameter  $\beta$  increases, the PAPR decreases considerably. As shown in the figures, the PAPR is reduced from 8 dB to 4.5 dB when the probability of the given threshold is  $10^{-4}$ . Also, Fig. 11 shows the PSD as  $\beta$  changes. Better results are achieved using MSNT than using the conventional OFDM technique, and there is no sensitivity to  $\beta$  variations in the PSD.

In the next step, we show the effect of the modulation type and number of subcarriers on the obtained results. As shown in Fig. 12, we apply MSNT by using several modulation types, such as QPSK, 16QAM, 64QAM, and 128QAM, assuming  $N = 64$  and  $N = 128$ ,  $\alpha = 0.2$ , and  $\beta = 10$ . The obtained result for PAPR is plotted in the figure. It is apparent that when the order of the modulation type increases and when  $N$  increases, the PAPR parameter decreases about 2 dB and the PAPR parameter improves about 1 dB, respectively.

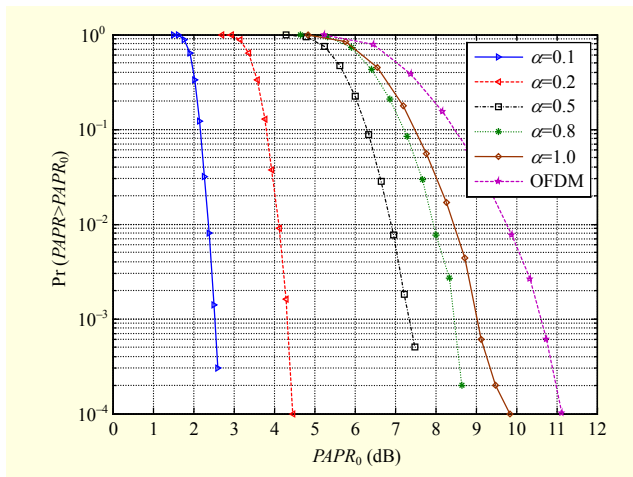


Fig. 8. CCDF of PAPR in MSNT; 64QAM,  $N=64$ ,  $L=16$  and  $\beta=10$ .

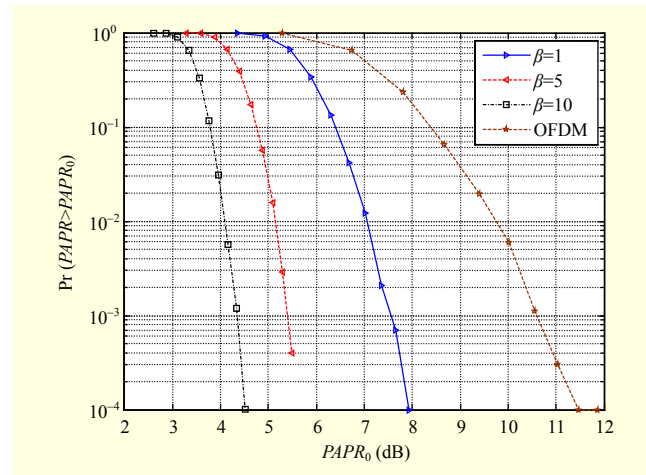


Fig. 10. CCDF of PAPR in MSNT; 64QAM,  $N = 64$ ,  $L=16$  and  $\alpha = 0.2$ .

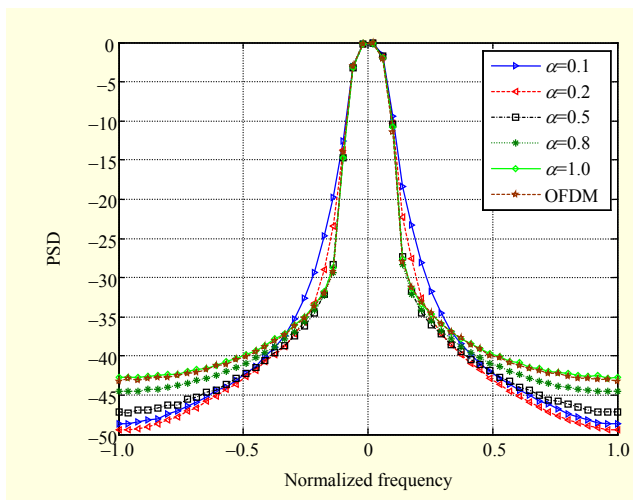


Fig. 9. PSD in MSNT; 64QAM,  $N = 64$ ,  $L=16$  and  $\beta=10$ .

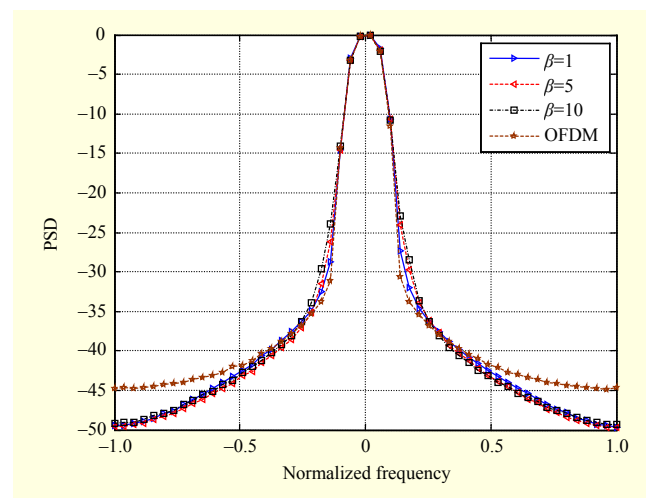


Fig. 11. PSD in MSNT; 64QAM,  $N = 64$ ,  $L=16$  and  $\alpha = 0.2$ .

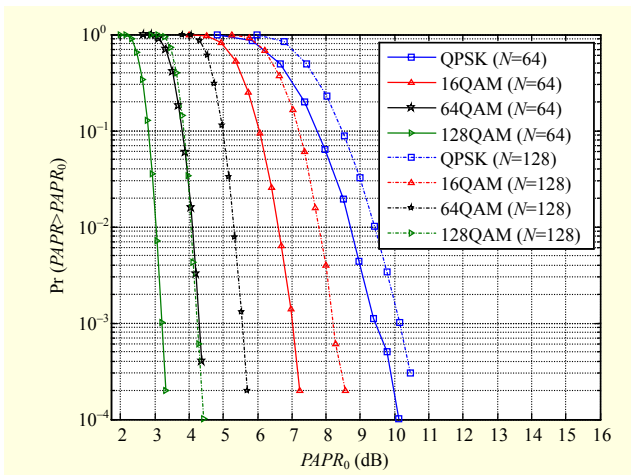


Fig. 12. CCDF of PAPR in MSNT with different modulation techniques;  $N=64$ , 128QAM,  $L=16$  and  $\alpha=0.2$ ,  $\beta=10$ .

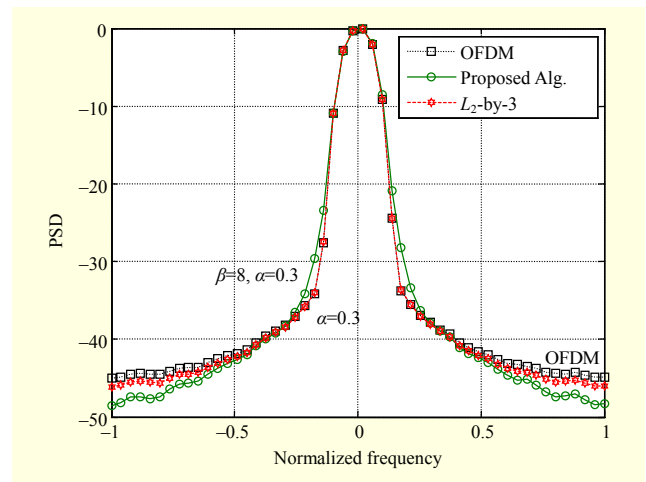


Fig. 14. Comparison of PSD between MSNT and other algorithms; 128QAM,  $N = 64$  subcarriers  $\alpha = 0.3$  and  $\beta = 8$ , and  $L=16$ .

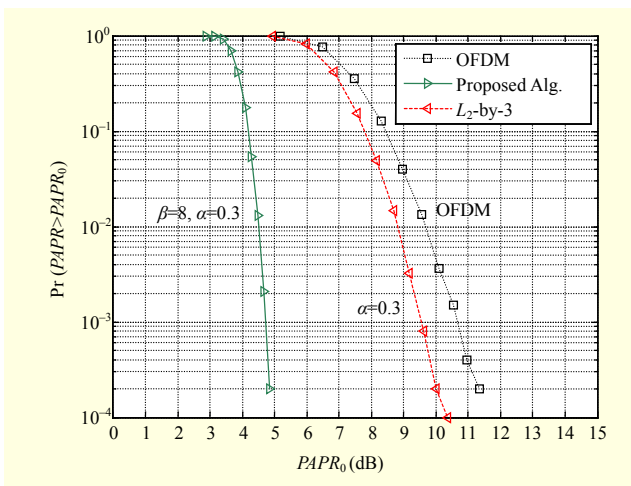


Fig. 13. Comparison of CCDF between MSNT and other algorithms; 128QAM,  $N = 64$  subcarriers  $\alpha = 0.3$  and  $\beta = 8$ , and  $L=16$ .

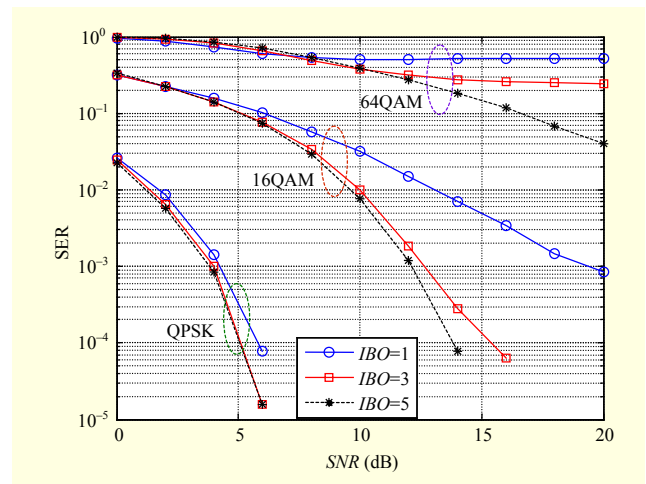


Fig. 15. SER in MSNT;  $N = 64$ ,  $\alpha = 0.2$ , and  $\beta=10$ .

For further evaluation, we compare the CCDF and PSD of MSNT with those of the conventional OFDM and  $L_2$ -by-3 algorithms, as shown in Figs. 13 and 14. In this evaluation, the baseband modulation is 128QAM and the  $N = 64$ . As shown in the figures, our algorithm obtains the best results in terms of PAPR reduction and PSD. For example, there is an approximately 5-dB reduction in the PAPR parameter when we have the same conditions as in the other methods, and desirable results are obtained regarding PSD, as shown in Fig. 14.

One of the most important problems in an OFDM system are in-band and out-of-band distortions, which can be created by a nonlinear HPA; therefore, there is BER performance degradation and spectral outgrowth. These distortions are related to the level of the backoff parameter in an HPA. Therefore, to investigate the BER performance of an OFDM

system based on MSNT, the OFDM signal with assumed values of  $\alpha$  and  $\beta$  is transmitted through the PA with different input backoff levels. The applied PA model in the simulation is the Rapp model.

The SER performance of MSNT with an AWGN channel nonlinear Rapp model HPA is considered. The PA parameters are  $IBO = 1$  dB, 3 dB, and 5 dB,  $V_{sat} = 0.5$ , and smoothing factor  $s = 5$ . After passing the OFDM symbol from the nonlinear amplifier, it is sent to the receiver through an AWGN channel in which the SNR can vary from 0 dB to 20 dB. The SER is calculated for two cases: two MSNT blocks and one MSNT block, both on the transmitter side and the receiver side. First, we consider the effect of various modulation schemes, including QPSK, 16QAM, and 64QAM, in which  $N = 64$  subcarriers are used, and we tune MSNT parameters  $\alpha$  and  $\beta$  to 0.2 and 10, respectively, with two MSNT blocks. The

Table 2. Complexity of proposed algorithm and  $L_2$ -by-3.

Methods	Addition complexity	Multiplication complexity
$L_2$ -By-3	$6(N-1)$	$6(N-1)$
MSNT with 2 MSNT block	$8(N-1)$	$10(N-1)$
MSNT with 1 MSNT block	$4(N-1)$	$5(N-1)$

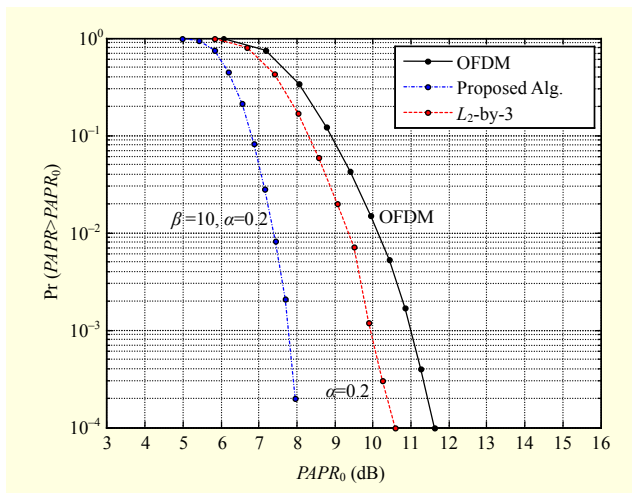


Fig. 16. Comparison of CCDF between MSNT and other algorithms; 128QAM,  $N = 64$  subcarriers  $\alpha = 0.3$  and  $\beta = 8$ ,  $L=16$ , and one MSNT block.

obtained results with the mentioned assumptions are plotted in Fig. 15. It is noticeable that when the order of modulation is decreased, the obtained results are remarkable; for example, in the case of the QPSK modulation, an SNR of approximately 4 dB is required to obtain an SER probability of  $10^{-3}$ . Also, it is noticeable that in the QPSK modulation, the error probability is not sensitive to the IBO variation.

## VI. Complexity Analysis

Another evaluation of our proposed method is a complexity analysis. Considering (10) and (13), anyone can compute the complexity of the mentioned algorithms with respect to the number of additions and multiplications of real numbers. In any MSNT subblock, we need five real multiplications and four real additions. In our proposed method, we use an MSNT subblock twice; therefore, we need  $10(N-1)$  real multiplications and  $8(N-1)$  real additions in any OFDM symbols that include  $N$  samples. If there is only one MSNT block in our proposed algorithm, then the multiplication and addition complexity is  $5(N-1)$  and  $4(N-1)$ , respectively. The

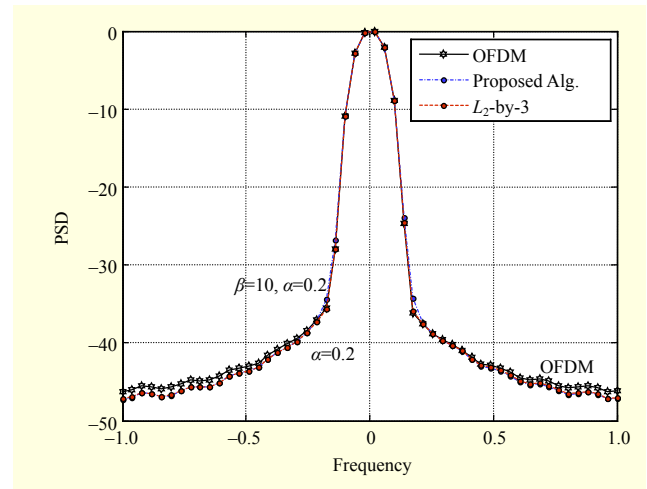


Fig. 17. Comparison of PSD between MSNT and other algorithms; 128QAM,  $N = 64$ ,  $\alpha = 0.3$ ,  $\beta = 8$ ,  $L = 16$ , and one MSNT block.

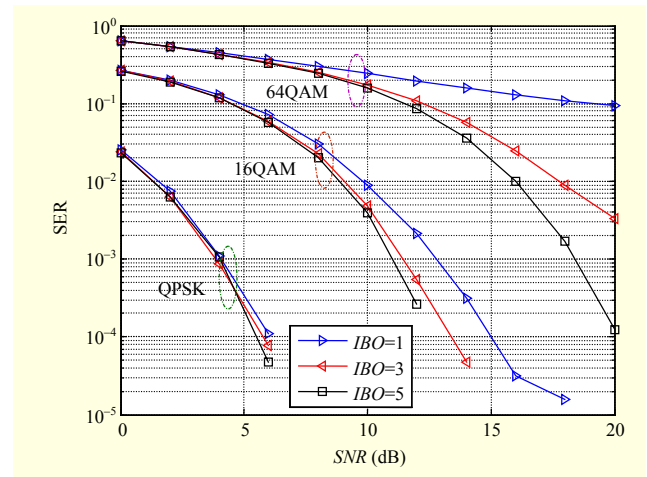


Fig. 18. SER in MSNT;  $N = 64$ ,  $\alpha = 0.2$ ,  $\beta = 10$ , and one MSNT block.

number of additions and multiplications of both algorithms are listed in Table 2. As shown in the table, our proposed algorithm has high complexity with respect to the  $L_2$ -by-3 algorithm when we use two MSNT blocks, but there is better performance in PAPR reduction and PSD. If anyone uses only one MSNT block in the MSNT algorithm, there is desirable performance in PAPR reduction. Figures 16 and 17 show the performance when only one MSNT block is used. In Fig. 18, the SER is plotted. In our future work, we want to simplify the proposed block diagram to have less complexity in the obtained results when there are two MSNT subblocks.

## References

- [1] S.B. Weinstein and P.M. Ebert, "Data Transmission by Frequency-



- Division Multiplexing Using the Discrete Fourier Transform,” *IEEE Trans. Commun. Technol.*, vol. 19, no. 5, Oct. 1971, pp. 628-634.
- [2] M. Breiling, S.H. Muller, and J.B. Huber, “SLM Peak-Power Reduction without Explicit Side Information,” *IEEE Commun. Lett.*, vol. 5, no. 6, June 2001, pp. 239-241.
- [3] S.H. Muller et al., “OFDM with Reduced Peak-to-Average Power Ratio by Multiple Signal Representation,” *Ann. Telecommun.*, vol. 52, no. 1-2, Feb. 1997, pp. 58-67.
- [4] S.H. Muller and J.B. Huber, “OFDM with Reduced Peak-to-Average Power Ratio by Optimum Combination of Partial Transmit Sequences,” *Electron. Lett.*, vol. 33, issue 5, Feb. 1997, pp. 368-369.
- [5] L.J. Cimini and N.R. Sollenberger, “Peak-to-Average Power Ratio Reduction of an OFDM Signal Using Partial Transmit Sequences,” *IEEE Commun. Lett.*, vol. 4, no. 3, Mar. 2000, pp. 86-88.
- [6] B.R. Saltzberg, “Performance of an Efficient Parallel Data Transmission System,” *IEEE Trans. Commun.*, vol. 15, no. 6, Dec. 1967, pp. 805-811.
- [7] R.W. Chang and R.A. Gibby, “A Theoretical Study of Performance of an Orthogonal Multiplexing Data Transmission Scheme,” *IEEE Trans. Commun.*, vol. 16, no. 4, Aug. 1968, pp. 529-540.
- [8] H.S. Hee and L.J. Hong, “An Overview of Peak-to-Average Power Ratio Reduction Techniques for Multicarrier Transmission,” *IEEE Wireless Commun.*, vol. 12, no. 2, Apr. 2005, pp. 56-65.
- [9] B.S. Krongold and D.L. Jones, “PAR Reduction in OFDM via Active Constellation Extension,” *IEEE Trans. Broadcast.*, vol. 49, no. 3, Sept. 2003, pp. 258-268.
- [10] Y.J. Kou, W.S. Lu, and A. Antoniou, “A New Peak-to-Average Power-Ratio Reduction Algorithm for OFDM Systems via Constellation Extension,” *IEEE Trans. Wireless Commun.*, vol. 6, no. 5, May 2007, pp. 1823-1832.
- [11] E. Jones, T.A. Wilkinson, and S.K. Barton, “Block Coding Scheme for Reduction of Peak to Mean Envelope Power Ratio of Multicarrier Transmission Schemes,” *Elect. Lett.*, vol. 30, no. 25, Dec. 1994, pp. 2098-2099.
- [12] A.E. Jones and T.A. Wilkinson, “Combined Coding for Error Control and Increased Robustness to System Nonlinearities in OFDM,” *Proc. IEEE VTC*, Atlanta, GA, USA, Apr.- May 1996, pp. 904-908.
- [13] S.C. Thompson, J.G. Proakis, and J.R. Zeidler, “The Effectiveness of Signal Clipping for PAPR and Total Degradation Reduction in OFDM Systems,” *Proc. IEEE Global Telecommun. Conf.*, Dec. 2005, pp. 2807-2811.
- [14] Tao Jiang and Guangxi Zhu, “Nonlinear Companding Transform for Reducing Peak-to-Average Power Ratio of OFDM Signals,” *IEEE Trans. Broadcast.*, vol. 50, issue 3, Sept. 2004, pp. 342-346.
- [15] Tao Jiang et al., “Two Novel Nonlinear Companding Schemes with Iterative Receiver to Reduce PAPR in Multicarrier Modulation Systems,” *IEEE Trans. Broadcast.*, vol. 52, issue 2, June 2006, pp. 268-273.
- [16] R.J. Baxley and G.T. Zhou, “Power Savings Analysis of Peak-to-Average Power Ratio in OFDM,” *IEEE Trans. Consum. Electr.*, vol. 50, no. 3, Aug. 2004, pp. 792-798.
- [17] S. Dursun and M.G. Artyom, “Nonlinear  $L_2$ -by-3 Transform for PAPR Reduction in OFDM Systems,” *Comput. Electr. Eng.*, vol. 36, no. 6, Nov. 2010, pp. 1055-1065.



**R. Salmanzadeh** was born in Tabriz, Iran, in 1987. He received his MS degree in wireless communications from the University of Tabriz. His research interests are in the area of wireless communications.



**B. Mozaffari Tazehkand** was born in 1968 in Iran. He received his BS degree in 1993 from the University of Tabriz and his MS degree in 1996 from K.N. Toosi University of Technology. Also, he received his PhD degree in 2006 from the University of Tabriz. His research interests are wireless communication, OFDM systems, and signal processing for communication systems.